Libraries of Statistical Hydroxypropyl Acrylate Containing Copolymers with LCST Properties Prepared by NMP

Tamara M. Eggenhuisen,[†] C. Remzi Becer,[†,‡,§] Martin W. M. Fijten,[†,§] Rebecca Eckardt,[†,§] Richard Hoogenboom,*[,†,§] and Ulrich S. Schubert*[,†,‡,§]

Laboratory of Macromolecular Chemistry and Nanoscience, Eindhoven University of Technology, Den Dolech 2, 5600 MB Eindhoven, The Netherlands; Laboratory of Organic and Macromolecular Chemistry, Friedrich-Schiller-University Jena, Humboldtstrasse 10, 07743 Jena, Germany; and Dutch Polymer Institute (DPI), John F. Kennedylaan 2, 5612 AB Eindhoven, The Netherlands

Received March 3, 2008; Revised Manuscript Received May 9, 2008

ABSTRACT: The nitroxide-mediated copolymerization of 2-hydroxypropyl acrylate (HPA) with *N*-acryloylmorpholine (Amor) or *N,N*-dimethylacrylamide (DMA) was investigated using *N*-*tert*-butyl-*N*-(1′-diethylphosphono-2,2′-dimethylpropyl)-*O*-(2-carboxyl-prop-2-yl) (BlocBuilder) alkoxyamine initiator and additional free nitroxide (SG-1). Different reaction conditions, such as the concentration of additional SG-1, were tested to optimize the homopolymerizations using a Chemspeed ASW2000 automated parallel synthesizer. Best control for the homopolymerizations (polydispersity indices of 1.2−1.3) of all three monomers was achieved using 20% additional SG-1 (relative to the initiator) at a reaction temperature of 110 °C for 2 M solutions in *N,N*-dimethylformamide and a monomer/initiator ratio of 100/1. Libraries of P(Amor-*stat*-HPA) and P(DMA-*stat*-HPA) were synthesized with 0−100 mol % HPA with 10 mol % increments using the optimized conditions obtained for the homopolymerizations. The resulting polymers had narrow molecular weight distributions, and their compositions, determined using ^{1}H NMR spectroscopy and elemental analysis, were close to the theoretical compositions. In addition, all copolymers of both libraries had single glass transition temperatures (T_g), and the transition temperatures decreased from the T_g of P(Amor) (147 °C) and P(DMA) (111 °C) to the T_g of P(HPA) (22 °C) with increasing HPA content. The cloud point of P(HPA) showed concentration dependence as well as a concentration dependent hysteresis. The cloud points of aqueous solutions of the copolymer libraries could be tuned from 21.4 to 88.0 °C and to 82.9 °C for P(Amor-*stat*-HPA) and P(DMA-*stat*-HPA), respectively, at a concentration of 1 wt %. LCST behavior was observed for copolymers with >40 wt % HPA in P(Amor-*stat*-HPA) and >55 wt % HPA in the P(DMA-*stat*-HPA) library.

Introduction

Polymers with a lower critical solution temperature (LCST) show a reversed solubility profile in water; i.e. the polymers precipitate upon heating and dissolve with cooling. At temperatures below the LCST, the polymer chains are hydrated and form hydrogen bonds with water molecules. Weakening of the hydrogen bonds at higher temperatures causes entropy-driven phase transition of the polymer to a hydrophobic collapsed state.[1] Such thermoresponsive polymers are of major interest for biotechnological applications,[2–4] including tissue engineering,[5] biomolecule separation,[6,7] and drug delivery systems,[8] but are also of interest for industrial applications in catalysis[9,10] or membranes.[11,12]

Since the phase transition temperature is directly related to the hydrophilic/hydrophobic balance in a (random co)polymer, controlling the polymer composition provides a very effective way of tuning the LCST.[1] By creating systematic libraries of random copolymers, the relationship between monomer composition and LCST can be studied in detail.[13–15] The most widely studied thermoresponsive polymer is poly(*N*-isopropylacrylamide) (P(NIPAM)), which has been known since 1956 and still attracts much attention, because its LCST of 32 °C is close to physiological conditions and the phase transition shows little concentration dependence.[16,17] A surprisingly little studied polymer with LCST behavior is poly(2-hydroxypropyl acrylate) (P(HPA)), with a reported LCST of 16 °C at 10 wt %.[1] Although its thermosensitivity was already reported in 1975,[1] other appearances in the literature are limited to the use of HPA as a comonomer in thermoresponsive hydrogels.[18,19] Because of the low LCST of P(HPA), copolymerization with a more hydrophilic monomer should lead to a library that covers a broad range of transition temperatures.

A narrow molecular weight distribution is an important prerequisite to create polymers with sharp LCST transitions.[20] Controlled radical polymerization techniques, such as atom transfer radical polymerization,[21,22] reversible addition fragmentation chain transfer (RAFT),[24] and nitroxide-mediated radical polymerization (NMP),[25,26] provide access to a large collection of monomers that can be polymerized in a controlled manner.[27,28] NMP was chosen for the present study as the development of acyclic phosphonylated nitroxides like *N*-*tert*-butyl-*N*-(1′-diethylphosphono-2,2′-dimethylpropyl) nitroxide (SG-1)[29,30] and corresponding highly reactive alkoxyamine initiators, such as the *N*-*tert*-butyl-*N*-(1′-diethylphosphono-2,2′-dimethylpropyl)-*O*-(2-carboxyl-prop-2-yl) alkoxyamine initiator (BlocBuilder initiator,[31] registered trademark of Arkema, Scheme 1), greatly improved the versatility, rate, and efficiency of this polymerization method.[32–37] The polymerization rates of highly reactive monomers can be tuned using additional free nitroxide, and controlled polymerization of styrenics, acrylates, and acrylamides was already demonstrated.[32,38,39] Furthermore, the controlled NMP of methacrylates using Blocbuilder could be performed in the presence of a small amount of styrene.[36]

Scheme 1 displays the structure of HPA and the selected hydrophilic comonomers, *N*-acryloylmorpholine (Amor) and *N,N*-dimethylacrylamide (DMA). Although controlled radical polymerization of HPA via RAFT was recently reported (polymerization at 80 °C in *tert*-butanol yielded polymers with

* Corresponding authors. E-mail: u.s.schubert@tue.nl or r.hoogenboom@tue.nl.
† Eindhoven University of Technology.
‡ Friedrich-Schiller-University Jena.
§ Dutch Polymer Institute.

10.1021/ma800469p CCC: $40.75
Published on Web 06/25/2008

Scheme 1. Schematic Representation of the Chemical Structures of BlocBuilder Alkoxyamine Initiator, SG-1 Free Nitroxide, and the Monomers *N,N*-Dimethylacrylamide, *N*-Acryloylmorpholine, and 2-Hydroxypropyl Acrylate

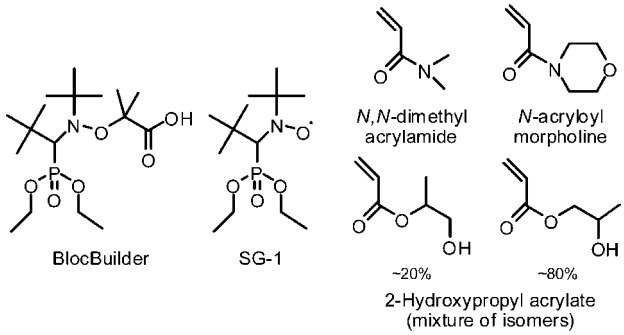

a polydispersity index of 1.08),[40] the NMP of HPA has not been reported. However, controlled NMP of hydroxyethyl acrylate using SG-1 has been described.[41,42] Amor has been reported as a comonomer in LCST polymers using both free radical[43] and RAFT polymerization procedures.[44–46] Successful NMP of Amor has only been described in a copolymerization with styrene using hydroxy-TEMPO while the homopolymerization was uncontrolled.[47] DMA was added to the present library as it is a well-known comonomer for LCST applications in combination with acrylates,[48,49] styrene,[50] and other acrylamides.[51–53] Controlled NMP of DMA has also been reported with various nitroxide initiators (bulk polymerization at 125 °C resulting in P(DMA) with a PDI < 1.10 without addition of free nitroxide)[48,54] as well as with 2,2′-azobis(isobutyronitrile)/SG-1 free nitroxide (bulk polymerization at 110 °C resulting in polymers with PDI < 1.20).[55,56] In addition, the controlled statistical copolymerization of DMA with methyl methacrylate was reported using BlocBuilder/SG-1.[57]

In this work, we access a new group of polymers with tunable LCST by copolymerizing HPA with Amor or DMA. In doing so, we add HPA and Amor to the already vast collection of monomers that can be polymerized in a controlled manner using the BlocBuilder initiator in NMP. In order to facilitate kinetic investigations and to create copolymer libraries for studying structure−property relationships, a high throughput experimentation setup was used.[58]

Experimental Section

Synthesis. *N,N*-Dimethylacrylamide (99%, Aldrich), *N*-acryloylmorpholine (97%, Aldrich), and 2-hydroxypropyl acrylate (mixture of isomers (Scheme 1), 95%, Aldrich) were filtered through a neutral alumina oxide column and stored in a refrigerator at 4 °C. All solvents were obtained from Biosolve and used as received. BlocBuilder initiator and SG-1 (85%) free nitroxide were kindly provided by Arkema and used as received.

All polymerizations were performed in a Chemspeed ASW2000 automated parallel synthesizer.[59] The used reactor block consists of 16 parallel 13 mL vessels, each equipped with a coldfinger reflux condenser controlled by a Huber Ministat in a temperature range of −5 to 45 °C. The reaction temperature was regulated through a heating jacket connected to a Huber Unistat 390 W cryostat with a temperature range of −90 to 150 °C. Agitation of the vessels was achieved by a vortex movement of the reactor block at 500 rpm. Two separately controlled argon flows were applied to flush the hood of the synthesizer robot and to maintain an argon atmosphere in the reactor block and over the stock solutions.

Homopolymerizations. An inert atmosphere in the Chemspeed ASW2000 hood was achieved by a 45 min flushing step with a 1.5 bar argon flow. The reaction vessels were heated to 120 °C and subjected to vacuum−argon cycles (0.1−1.1 bar) for 3 min, which were repeated three times to create an inert atmosphere. The monomer *N,N*-dimethylformamide (DMF) and stock solutions of the BlocBuilder initiator and free SG-1 in DMF were degassed prior to the reaction by bubbling with argon for at least 25 min. The monomer, stock solutions, and solvent were automatically transferred to the reaction vessels in the predefined volumes leading to a total reaction volume of 4 mL. The monomer concentration was 2 M, and the monomer/initiator ratio was 100/1 with variable amounts of additional SG-1 free nitroxide. The reactor block was heated to 110 or 120 °C for the predefined reaction time. After the temperature was reached, 100 μL samples were transferred to empty sample vials at set time intervals, after which 0.8 mL of chloroform was added to dilute the sample. The samples were analyzed with gas chromatography (GC) and gel permeation chromatography (GPC) to determine the reaction kinetics. For manual precipitation of the final polymers, the reaction mixtures were diluted with 4 mL of $CHCl_3$ and added dropwise to a vigorously stirred 10-fold excess of diethyl ether. P(DMA) and P(Amor) were isolated by filtration while P(HPA) was left to settle followed by decantation. The polymers were dried in a vacuum oven at 40 °C until no residual solvent was observed by ^{1}H NMR spectroscopy.

Copolymerizations. The copolymerizations were performed using the same setup as the homopolymerizations. The two monomers were added in different ratios, resulting in monomer mixtures ranging from 0 to 100 mol % HPA with 10 mol % increments. The total monomer concentration was 2 M, and the monomer/initiator/SG-1 ratio was 100/1/0.2. The reaction temperature was set to 110 °C, and the reaction times were chosen to reach ∼60% monomer conversion. The 100 μL zero time and end samples were automatically transferred to empty vials and diluted with 0.8 mL of $CHCl_3$ to determine monomer conversion with GC. Precipitation of the copolymers was achieved following the same procedure as for the homopolymers. A second precipitation was applied, if necessary, to remove residual DMF and monomer. The final polymers were analyzed by GPC, ^{1}H NMR spectroscopy, and elemental analysis.

Characterization Techniques. GPC was performed on a Shimadzu system with a SCL-10A system controller, a LC-10AD pump, a RID-10A refractive index detector, and PSS gram 30 (pore size 30 Å; bead size 10 μm; 100−10 000 Da) and PSS gram 1000 (pore size 1000 Å; bead size 10 μm; 1000−1 000 000 Da) columns in series at 60 °C. A solution of *N,N*-dimethylacetamide (DMAc) containing 2.1 g of LiCl/L was used as an eluent at a flow rate of 1 mL/min. The average molecular weights were calculated against poly(methyl methacrylate) (P(MMA)) calibration standards. GC was used to calculate the monomer conversion through the decreasing monomer/DMF ratio in the samples. Measurements were performed on an Interscience Trace GC equipped with a PAL autosampler, an Interscience liner for injecting polymers (injection temperature of 250 °C), a Trace Column RTX-5, and a FID detector at 275 °C. The following temperature program was used for the column oven: hold for 2 min at 50 °C, ramp from 50 to 150 °C (30 °C/min), ramp from 150 to 300 °C (50 °C/min), and hold for 1 min at 300 °C.

Composition and purity of the polymers were determined using ^{1}H NMR spectroscopy. The composition of the copolymers was determined using the integrals of HPA at 4.9 ppm (C*H*O of the minor isomer) and 3.0−4.0 ppm (CH_2O both isomers and C*H*O of the major isomer), the integral of Amor at 3.2−4.0 ppm (CH_2N and CH_2O), and the integral of DMA at 2.9 ppm (CH_3). Spectra were recorded on a Varian Mercury 400 MHz spectrometer in $CDCl_3$. The residual protonated solvent signals were used as reference. Elemental analysis (EA) was performed on a Hekatech EA3000 EuroVector CHNS analyzer. The determined wt % N was used to calculate the molar content of DMA monomer and BlocBuilder initiator (which was approximated as $1/DP_{DMA}$ from the GC conversion; the attributed nitrogen content from the added SG-1 was neglected). The remaining carbon content was ascribed to the HPA monomer, leading to the HPA wt % in the copolymers. Using this method, the combined wt % of DMA, BlocBuilder

initiator, and HPA was 100 ± 6%, and the calculated wt % H was within 0.1% of the measured value.

Thermal transitions were determined by differential scanning calorimetry (DSC) using a DSC 204 F1 Phoenix by Netzsch (calibrated using Netzsch standards). Each measurement consisted of two heating cycles to 200 °C under a nitrogen flow. In the first cycle, heating to 200 °C and subsequent cooling to −100 °C occurred at a rate of 40 °C/min. The second cycle was used to determine the transition temperatures and was performed at a heating rate of 20 °C/min. The glass transitions were determined from the mid-temperature of the transition.

The cloud points were determined by turbidity measurements in a Crystal 16 by Avantium Technologies. Four blocks of four parallel temperature-controlled sample holders are connected to a Julabo FP40 cryostat, allowing 16 simultaneous measurements. Turbidity of the solutions was measured by the transmission of a red light through the sample vial as a function of the temperature. Solutions of the polymers were prepared in deionized water (Laborpure, Behr Labor Technik) and were stirred at room temperature until all polymer was dissolved or dispersed. Three or four heating cycles were applied from 0 to 100 °C at 1 °C/min with hold steps of 5 min at the extreme temperatures. The cloud points are given as the 50% transmittance point during the first heating ramp.

Results

Homopolymerizations. A kinetic investigation was conducted for the homopolymerizations of Amor, DMA, and HPA to establish optimal reaction conditions for the synthesis of statistical copolymers based on these monomers. The use of a Chemspeed ASW2000 synthesis robot allowed rapid screening of important reaction parameters, such as the solvent, temperature, and free nitroxide concentration. The previously obtained optimal conditions for the NMP of *tert*-butyl acrylate were taken as a starting point: toluene as solvent, 110 °C polymerization temperature, and SG-1 percentages up to 10% relative to the alkoxyamine initiator.[60] Since P(Amor) is insoluble in toluene, DMF was taken as a more polar solvent, which is known to increase the polymerization rate in NMP.[61] Temperatures of 110 and 120 °C were tested with SG-1 percentages up to 20%. Increased polymerization rates were obtained at 120 °C, reducing the reaction times, but none of the polymerizations revealed good control, even with 20% additional SG-1. Therefore, all further reactions were performed at 110 °C. Other reaction conditions were kept constant using a 2 M monomer concentration and a monomer/initiator ratio of 100 to 1. For the kinetic investigations, nine aliquots were withdrawn from the polymerization mixtures at set intervals during 15 h to determine the monomer conversions, average molecular weights, and polydispersity indices.

Figure 1 shows the optimization of the additional SG-1 percentage at 110 °C in DMF for all three monomers. Linear first-order kinetics was observed for all three monomers at different SG-1 percentages, indicating a constant concentration of propagating radicals under these conditions. The increasing molecular weights with conversion and progression of the monomodal GPC traces in time (see Figure 2) further confirmed the control over the polymerizations.

Addition of 20% SG-1 resulted in improved control and PDI values in the range of 1.2−1.3 for conversions up to at least 60%. In the case of DMA, 20% SG-1 resulted in similar control as 15%, while for the other two monomers an increase in control could still be observed. Nevertheless, 20% SG-1 was taken as the optimum as it led to the desired control, while still a reasonable conversion could be obtained within 15 h reaction time.

Amor revealed the highest polymerization rates without additional SG-1, but the polydispersity indices demonstrated poorly controlled polymerization (see Figure 1A,B). With the addition of free nitroxide, the polymerization rate decreased due to the presence of more dormant species and thus a lower free radical concentration. The lower concentration of free radicals results in less termination reactions leading to the necessary increase in control. With the addition of 20% SG-1, PDI values in the range from 1.2 to 1.3 were obtained for a conversion up to 80%. For all investigated Amor polymerizations with additional SG-1, the M_n increased linearly with the conversion with a lower slope than the theoretical M_n. In general, there is most likely a discrepancy between the hydrodynamic volume of P(Amor) and the P(MMA) calibration used for calculating the molecular weights. In addition, the occurrence of some chain transfer and/or autoinitiation reactions may result in lower molecular weights than the expected values.

Similar to the results for Amor and to what has been reported in literature,[55–57] controlled polymerization of DMA was achieved by addition of SG-1 free nitroxide (see Figure 1C,D). Without the free nitroxide, a nonzero intercept in the semilogarithmic plot and PDI values of ∼1.6 were observed, indicating a relatively fast initiation and the occurrence of side reactions. Nonetheless, the desired level of control was obtained at 15% or 20% SG-1 with PDI values in between 1.20 and 1.25. The M_n values increased linearly with the conversion up to ∼75%. The slightly lower slope than for the theoretical M_n may result from similar effects as discussed previously for P(Amor).

Reaction conditions of 110 °C and 20% additional SG-1 also resulted in the best results for the homopolymerization of HPA (see Figure 1E,F). The M_n increased linearly with the conversion up to 60%, after which the M_n leveled off and the PDI values started to increase. Possible side reactions, such as chain transfer, autoinitiation, termination, and nitroxide decomposition, may cause the increased PDI values at higher monomer conversions. Therefore, reaction times should be limited to aim for 60% conversion of HPA to ensure good control over the polymerization. In addition, the M_n values obtained by GPC measurements seem to be overestimated using the P(MMA) calibration. Unfortunately, P(HPA) is not suitable for MALDI-TOF MS analysis, and end-group identification in ^{1}H NMR was not possible. However, the livingness of the polymerization was confirmed by the continuous progression of the GPC traces with time as presented in Figure 2. The monomer conversions were calculated as the sum of the two hydroxypropyl acrylate isomers.

From the slope of the first-order kinetic plots the apparent polymerization rate ($K_{p,app}$) was calculated for the optimal polymerization conditions, i.e., polymerization at 110 °C in DMF using a 2 M monomer concentration and 20% free SG-1 nitroxide. The polymerization of Amor was found to be the fastest, $K_{p,app} = 16.0 \times 10^{-4}$ L mol^{-1} s^{-1}, followed by DMA, $K_{p,app} = 7.7 \times 10^{-4}$ L mol^{-1} s^{-1}, and HPA was found to be the slowest monomer with a $K_{p,app}$ of 4.3×10^{-4} L mol^{-1} s^{-1}. This order in reactivity demonstrates that the acrylamides, DMA and Amor, are more reactive in NMP than the acrylate, HPA. These results also suggest that the hydroxyl group of HPA does not have a strong catalytic interaction with the nitroxide via hydrogen bonding, which was previously reported to accelerate the NMP.[62,63] The absence of such catalytic hydrogen bonding between the HPA and SG-1 might be due to the polar reaction medium, DMF, that suppresses the formation of hydrogen bonds. As a result of the different reactivity, the copolymerizations of these monomers will not yield ideal random copolymers but will most likely have a certain monomer gradient through the polymer chains.

Copolymerizations. The two hydrophilic monomers, Amor and DMA, were copolymerized with HPA to create two libraries with tunable LCST properties. The reaction conditions were chosen on the basis of the kinetic investigation of the homopolymerizations. For all three monomers good control was obtained

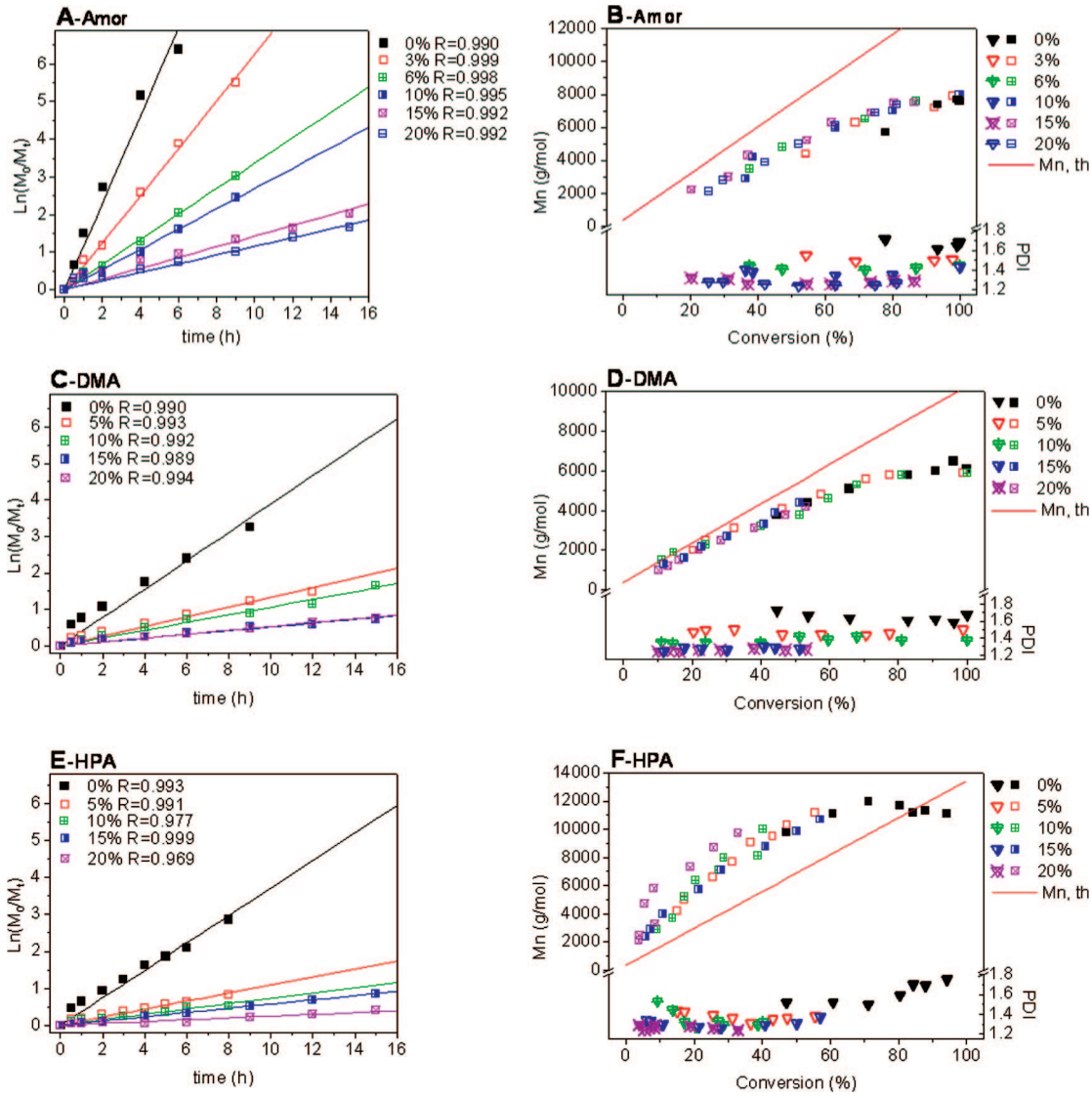

Figure 1. Kinetic investigation of the homopolymerizations of *N*-acryloylmorpholine (Amor; A and B), *N,N*-dimethylacrylamide (DMA; C and D), and 2-hydroxypropyl acrylate (HPA; E and F) with different percentages SG-1 (see legend of the graphs) at 110 °C in *N,N*-dimethylformamide at 2 M monomer concentration and a monomer-to-initiator ratio of 100. Left row: $\ln(M_0/M_t)$ vs time plots. Right row: Number-average molecular weight (M_n) and polydispersity index (PDI) vs conversion plots.

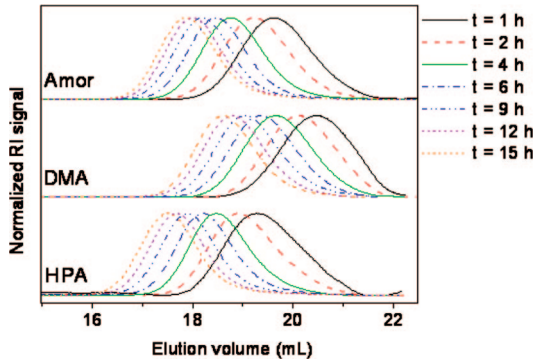

Figure 2. Gel permeation chromatography traces for the homopolymerizations of *N*-acryloylmorpholine (Amor), *N,N*-dimethylacrylamide (DMA), and 2-hydroxypropyl acrylate (HPA) in *N,N*-dimethylformamide with 20% SG-1 at 110 °C using 2 M monomer concentration and a monomer-to-initiator ratio of 100.

for 2 M DMF solutions at 110 °C and with 20% additional SG-1. Statistical copolymers of Amor with HPA and DMA with HPA were synthesized with varying monomer feed ratios from 0 to 100 mol % HPA with intervals of 10 mol % for both combinations. To achieve well-defined materials with narrow molecular weight distributions and thus sharp LCST transitions, reaction times of 8 and 15 h were used for the Amor and DMA library, respectively.

The copolymers obtained for the P(Amor-*stat*-HPA) library revealed relatively low polydispersity indices in the range from 1.16 to 1.32 and increasing M_n values with increasing HPA content (Table 1). This is in contradiction with the lower molecular weight of HPA and the lower conversions observed for the polymerizations with higher HPA contents in the monomer feed. However, this discrepancy can be ascribed to the use of the P(MMA) calibration and corresponds to the difficulties already encountered for the determination of the M_n of the homopolymers. The monomer conversions appear to be dependent on the composition of the monomer mixture. The observed polymerization rates for both monomers decreased with increasing HPA content. Apparently, the polymerization rate is dominated by the slower HPA-SG-1 dissociation and association kinetics. For A100 in Table 1, the conversion is calculated by ^{1}H NMR spectroscopy, since an error during automated sampling obstructed the GC analysis.

Table 1. Copolymerization Results of P(Amor-*stat*-HPA) Library (Amor = *N*-Acryloylmorpholine, HPA = 2-Hydroxypropyl Acrylate)

name[a]	conversion[b] (%)Amor/HPA	M_n[c] (g/mol)	PDI[c]	composition GC[b](mol %) Amor/HPA	composition NMR[d] (mol %) Amor/HPA
A100	70/0[e]	6900	1.32	100/0	100/0
A90H10	63/69	7700	1.27	89/11	90/10
A80H20	48/51	7200	1.22	79/21	78/22
A70H30	56/53	8300	1.26	71/29	68/32
A60H40	45/38	8100	1.21	64/36	58/42
A50H50	45/42	8500	1.23	52/48	47/53
A40H60	37/28	8300	1.20	47/53	38/62
A30H70	37/31	8800	1.20	34/66	29/72
A20H80	34/28	8400	1.20	23/77	18/82
A10H90	28/20	8100	1.16	13/87	7/93
H100	0/22	8200	1.16	0/100	0/100

[a] Names indicate monomer feed: A50H50 = P($Amor_{50}$-*stat*-HPA_{50}). [b] Calculated by gas chromatography (GC) using monomer/*N,N*-dimethylformamide ratios. [c] Number-average molecular weight (M_n) and polydispersity index (PDI) of the precipitated polymer determined by gel permeation chromatography. [d] ^{1}H NMR spectra were recorded in $CDCl_3$ (for details see Experimental Section). [e] Conversion calculated by ^{1}H NMR spectroscopy (signals of Amor at 5.6−6.6 ppm ($CH{=}CH_2$) and 3.6 ppm (CH_2N and CH_2O); signal of P(Amor) at 3.2−4.0 ppm (CH_2N and CH_2O).

Table 2. Copolymerization Results of P(DMA-*stat*-HPA) Library (DMA = *N,N*-Dimethylacrylamide, HPA = 2-Hydroxypropyl Acrylate)

name[a]	conversion[b] (%)DMA/HPA	M_n[c] (g/mol)	PDI[c]	composition NMR[d] (mol %) DMA/HPA	composition EA (mol %) DMA/HPA
D100	53/0	4500	1.23	100/0	100/0
D90H10	60/93	6800	1.20	85/15	88/12
D80H20	46/36	6500	1.23	75/25	78/22
D70H30	67/73	8400	1.27	69/31	68/32
D60H40	57/56	8500	1.24	53/48	59/41
D50H50	66/53	9800	1.27	46/54	50/50
D40H60	58/53	9600	1.26	33/67	41/59
D30H70	82/29	10900	1.24	28/72	32/68
D20H80	57/44	10700	1.22	18/82	22/78
D10H90	71/48	10500	1.20	9/91	12/88
H100	0/33	11100	1.21	0/100	0/100

[a] Names indicate monomer feed: D50H50 = P(DMA_{50}-*stat*-HPA_{50}). [b] Calculated by gas chromatography (GC) using monomer/*N,N*-dimethylformamide ratios. [c] Number-average molecular weight (M_n) and polydispersity index (PDI) of precipitated polymer; determined by gel permeation chromatography. [d] ^{1}H NMR spectra were recorded in $CDCl_3$ (for details see Experimental Section).

Copolymer compositions could be calculated from the GC conversion as well as ^{1}H NMR spectroscopy of the precipitated polymers. However, the latter method was complicated due to overlapping signals of the Amor side group ($-CH_2-$, δ = 3.1−3.9 ppm) and HPA signals ($-CH_2-$ and CH, δ = 3.4−4.2 ppm). Nevertheless, in both methods similar compositions were obtained and the ^{1}H NMR compositions were used to determine structure−property relationships for this library.

A reaction time of 15 h was used for the synthesis of the P(DMA-*stat*-HPA) library, which corresponds to 60% conversion in the homopolymerization of DMA and 47% conversion for HPA. The relatively low PDI values (1.20−1.27, Table 2) of the resulting polymers indicate a controlled copolymerization. The M_n of the copolymers increased with increasing HPA content as the HPA monomer has a larger molecular weight than DMA (MW_{HPA} = 130.14 g/mol and MW_{DMA} = 99.13 g/mol). In addition, the M_n of P(HPA) was also found to be overestimated using the P(MMA) calibration (see Figure 1F). It should be noted that the polymers have moderate molecular weights, and thus variation in chain length might influence the thermal and solution properties of these copolymers. Additional copolymerization attempts using longer reaction times revealed that higher molecular weight copolymers are also accessible using the optimized polymerization procedure.

The conversions of the copolymerization that were determined by GC analysis revealed an unexpected variation, which appears to represent a large error in the measurements. Interactions of this monomer combination with the glass polymer liner of the GC are thought to cause these errors. The alternative method, ^{1}H NMR spectroscopy, was also not suitable for reliable conversion determination since the DMA−CH_3 groups overlap not only with the HPA−O*H* group in the ^{1}H NMR spectra but also with broad backbone signals, which obstruct reliable integration. Because of the large uncertainty in the GC conversion and the ^{1}H NMR integration, elemental analysis was used as alternative method to calculate the molecular composition of the copolymers. The molar compositions resulting from EA are within 5% of the initial monomer feed independent of the monomer ratio, indicating a random incorporation of the monomers. Table 2 shows the compositions calculated according to the ^{1}H NMR analysis and elemental analysis.

Thermal Transitions. The thermal transitions of the two copolymer libraries were investigated using differential scanning calorimetry (DSC). For both libraries, single glass transition temperatures were observed which could be related to the monomer composition, indicating good mixing of the two polymers and/or a random monomer distribution. To further test the miscibility of the homopolymers, two blends of Amor/HPA and DMA/HPA were prepared. The blends showed a weak single glass transition that was within 10 °C of the glass transition of the corresponding copolymer with similar weight fractions of composition, demonstrating good miscibility of the homopolymers. For the thermal analysis, P(HPA) reacted for 15 h was used for both libraries, as the amount of isolated copolymer synthesized with 8 h of reaction time was not sufficient for proper analysis.

The transition temperatures for P(Amor-*stat*-HPA) and P(DMA-*stat*-HPA) as a function of the wt % HPA are displayed in Figure 3. For the Amor library, glass transitions temperatures were found to be in between 147 °C (for P(Amor)) and 22 °C (for P(HPA)) as listed in Table 3. The glass transition of D100 or P(DMA) was observed at 111 °C, and the glass transitions for the P(DMA-*stat*-HPA) copolymers, listed in Table 4, also revealed a relation to the wt % HPA in the temperature range of 111−22 °C. The Fox equation predicts the glass transition temperature of polymer blends or statistical copolymers via a reciprocal relation to the weight fraction of the composition and

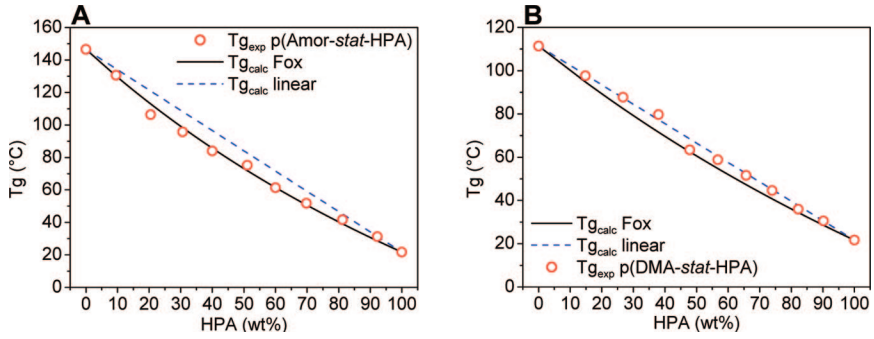

Figure 3. Glass transition temperature vs composition for the P(Amor-*stat*-HPA) library (A) and the P(DMA-*stat*-HPA) library (B). Amor = *N*-acryloylmorpholine, HPA = 2-hydroxypropyl acrylate, and DMA = *N,N*-dimethylacrylamide.

Table 3. Thermal Properties and Cloud Points for the Copolymers of the P(Amor-*stat*-HPA) Library (Amor = *N*-Acryloylmorpholine, HPA = 2-Hydroxypropyl Acrylate)

name	composition[a] Amor/HPA (wt %)	T_g[b] (°C)	cloud point[c] 0.5 wt % (°C)	cloud point[c] 1.0 wt % (°C)
A100	100/0	146.5	soluble	soluble
A90H10	90/10	130.6	soluble	soluble
A80H20	80/20	106.4	soluble	soluble
A70H30	69/31	95.8	soluble	soluble
A60H40	60/40	84.0	soluble	88.0
A50H50	49/51	75.2	79.5	65.9
A40H60	40/60	61.4	62.7	53.0
A30H70	30/70	51.8	49.2	38.3
A20H80	19/82	41.7	41.5	30.9
A10H90	8/82	31.3	33.9	25.3
H100[d]	0/100	21.7	26.7	21.4

[a] Calculated from ^{1}H NMR spectroscopy (for details see Experimental Section). [b] Mid-temperature. [c] 50% transmittance point in first heating curve. [d] P(HPA) synthesized with 15 h reaction time.

Table 4. Thermal and LCST Properties for the Copolymers of the P(DMA-*stat*-HPA) Library (DMA = *N,N*-Dimethylacrylamide, HPA = 2-Hydroxypropyl Acrylate)

name	composition[a] DMA/HPA (wt %)	T_g[b] (°C)	cloud point[c] 0.5 wt % (°C)	cloud point[c] 1.0 wt % (°C)
D100	100/0	111.4	soluble	soluble
D90H10	85/15	97.6	soluble	soluble
D80H20	73/27	87.7	soluble	soluble
D70H30	62/38	79.7	soluble	soluble
D60H40	52/48	63.4	soluble	soluble
D50H50	43/57	58.8	soluble	82.9
D40H60	34/66	51.6	71.6	62.3
D30H70	26/74	44.6	55.8	48.7
D20H80	18/82	36.0	46.7	38.6
D10H90	10/90	30.5	35.3	28.5
H100	0/100	21.7	26.7	21.4

[a] Calculated from elemental analysis. [b] Mid-temperature. [c] 50% transmittance point in first heating curve.

the transition temperature of the homopolymers.[64] However, polymers with specific interactions such as hydrogen bonding may show glass transition temperatures with a positive deviation from the Fox equation.[65–67] For P(Amor-*stat*-HPA), the glass transition temperatures correspond well to the Fox equation (Figure 3A). However, the glass transition temperatures of the P(DMA-*stat*-HPA) copolymers show a positive deviation with the Fox equation (Figure 3B). This indicates the presence of some weak hydrogen bonding of the HPA hydroxyl group with the amide group of DMA.

LCST Transitions. Since there are only few reports on the thermoresponsive behavior of P(HPA) in water,[1,40] the LCST of this polymer was determined at different concentrations. Figure 4 shows the transmittance as a function of the temperature for 0.25, 0.5, 1.0, and 1.5 wt % aqueous solutions. In this work, the 50% transmittance point in the first heating curve is taken as the cloud point, which ranges from 18.3 °C at 1.5 wt % to 33.3 °C at 0.25 wt % for P(HPA). Three important observations can be made from the curves in Figure 4. First, the LCST decreases with increasing polymer concentration—a behavior that is also observed for other LCST polymers at concentrations below 20 wt %.[68,69] Second, the transition becomes more diffuse

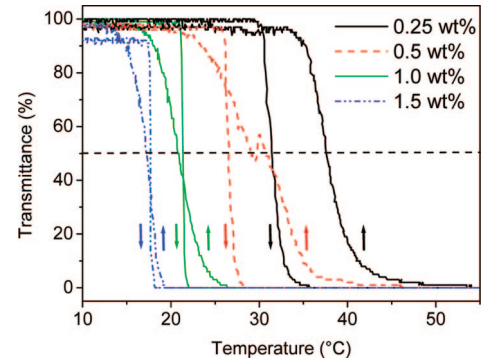

Figure 4. Transmittance as a function of temperature for poly(2-hydroxypropyl acrylate) (number-average molecular weight = 11 100, polydispersity index = 1.21) at different concentrations.

at low concentrations, especially in the dissolution curve. Finally, large hysteresis was observed at the lower concentrations with the redissolution occurring at higher temperatures than the precipitation. Since the size of the aggregates formed above the LCST is dependent on the concentration,[70] it appears that

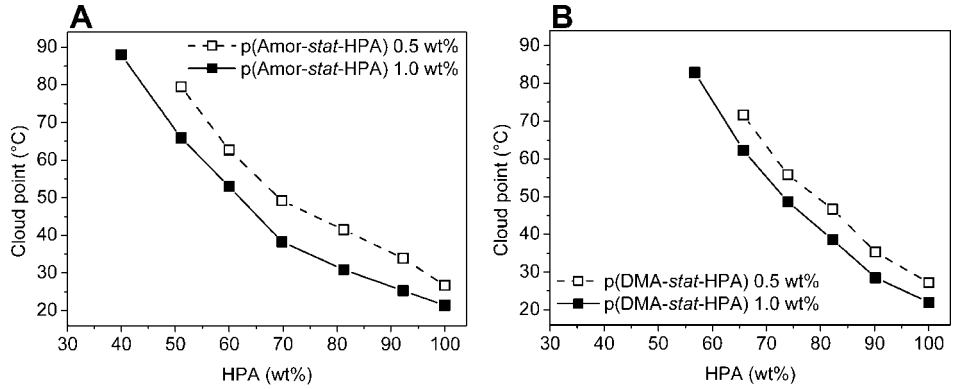

Figure 5. Cloud point as a function of polymer composition estimated by 50% transmittance points for first heating curves for P(Amor-*stat*-HPA) (A) and P(DMA-*stat*-HPA) (B). Amor = *N*-acryloylmorpholine, HPA = 2-hydroxypropyl acrylate, and DMA = *N,N*-dimethylacrylamide.

the intermolecular aggregation is less efficient for the lower concentrated samples. In addition, an incomplete aggregate formation could explain the higher dissolution temperature. Nevertheless, more detailed studies using FT-IR and/or DLS need to be performed in future work to provide a conclusive explanation for the observed behavior. It is worth noticing that the hysteresis observed is reversed from the hysteresis observed for P(NIPAM), where limited diffusion of water into the hydrophobic aggregates above the LCST retards the rehydration process.[71] This might indicate fast diffusion of water into the P(HPA) aggregates above the LCST.

The LCST behavior of the two copolymer libraries was studied at two different concentrations, 0.5 and 1.0 wt %. The observed cloud points are listed in Table 3 and Table 4. For both libraries the cloud points could be tuned between 20 and 100 °C. The 50% transmittance points of the first heating curve are displayed in Figure 5 as a function of the wt % HPA showing a clear decrease in cloud points with increasing HPA content. The cloud point dependence on the HPA content is comparable for 0.5 and 1.0 wt %, although the transitions in 0.5 wt % solutions occur ~10 °C higher. The P(Amor-*stat*-HPA) copolymers with >40 wt % HPA showed cloud points at 1.0 wt %, while at 0.5 wt % >55 wt % HPA was required. The more hydrophilic DMA monomer causes a slightly sharper increase in the LCST compared to Amor. For this library, the polymers with more than 55 wt % HPA showed LCST behavior at 1.0 wt % polymer concentration while 65 wt % HPA was required to find a cloud point at 0.5 wt % polymer concentration.

The transmittance drop of the first heating curve as a function of the temperature is displayed in Figure 6. Sharp transitions are observed for the polymers with high HPA contents similar to P(HPA) at 1.0 wt %. The polymers with higher hydrophilic content (i.e., A60H40 and D50H50 in parts A and B of Figure 6, respectively) show a more diffuse and incomplete transition. Copolymers of P(NIPAM) with more hydrophilic monomers also exhibited more diffuse transitions, which was ascribed to an inhibited collapse and aggregate formation by the smaller amount of dissociating water molecules.[52,72] During the cooling curves, a similar increase in transition time was observed (not shown). Before the LCST measurement, A20H80 was not fully dissolved, which explains the slightly lower transmittance at lower temperatures. The transmittance of the soluble polymers slightly decreases due to a change in the sensor sensitivity at higher temperatures.[73]

Typical turbidity curves of two heating cycles are displayed in Figure 7. Although the LCST transition is known to be reversible, copolymers with relatively high HPA contents became clear at all investigated temperatures after several heating cycles at low concentrations. Indeed, the curve of D50H50 reveals a noncomplete transmittance drop in the second

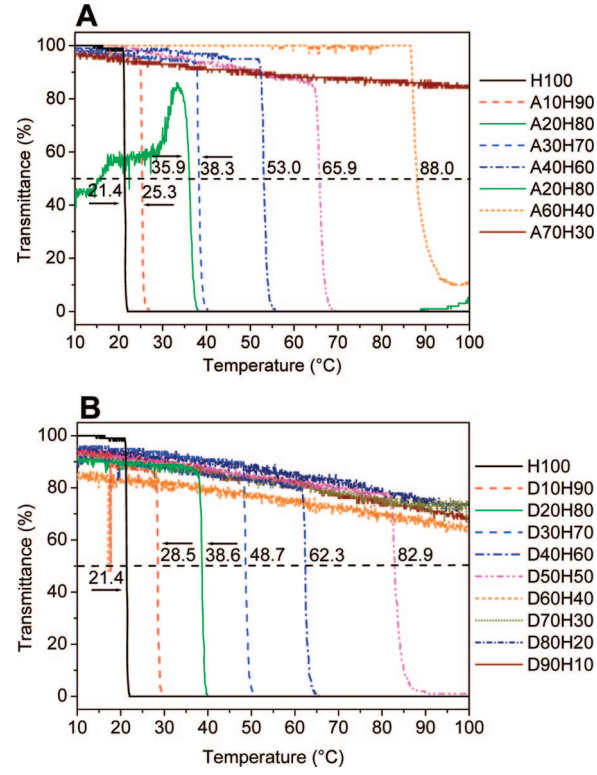

Figure 6. Transmittance as a function of temperature for 1.0 wt % aqueous solutions of P(Amor-*stat*-HPA) library (A) and P(DMA-*stat*-HPA) library (B). Amor = *N*-acryloylmorpholine, HPA = 2-hydroxypropyl acrylate, and DMA = *N,N*-dimethylacrylamide.

heating cycle. Figure 8A shows the 50% transmittance points for four heating and cooling cycles of different polymers from the P(DMA-*stat*-HPA) library at 1.0 wt %. The increase in LCST with increasing number of heating cycles is most apparent for D50H50, which is soluble after the second heating cycle. D40H60 exhibits an increase of 8 °C in the 50% transmittance point of the heating curve. For P(Amor-*stat*-HPA), similar observations were made. The increase in the cloud point for the copolymers with a high hydrophilic content became less noticeable at higher concentrations, as is shown for P($Amor_{40}$-*stat*-HPA_{60}) in Figure 8B. The temperature difference between precipitation and rehydration also decreases with increasing HPA content or increasing concentration.

The increase of the LCST and hysteresis depends on the concentration as well as the hydrophilic content in the copolymer. Therefore, there seems to be a relation of the observed hysteresis to the size and composition of the aggregates above

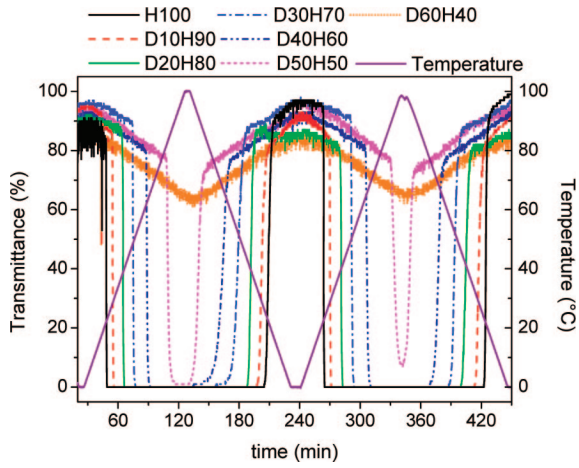

Figure 7. Transmittance curves as a function of time for copolymers of the P(DMA-*stat*-HPA) library. For clarity, the curves with <40% HPA have been left out. DMA = *N,N*-dimethylacrylamide and HPA = 2-hydroxypropyl acrylate.

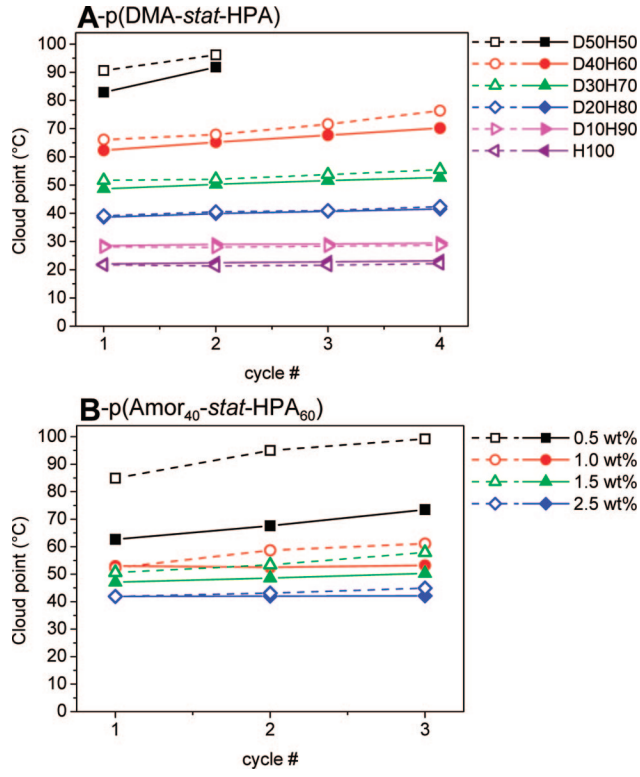

Figure 8. Cycle effect on cloud point determined as 50% transmittance points in heating curves (closed symbols) and cooling curves (open symbols) for different compositions of P(DMA-*stat*-HPA) at 1.0 wt % (A) and different concentrations of P(Amor$_{40}$-*stat*-HPA$_{60}$) (B). Amor = *N*-acryloylmorpholine, HPA = 2-hydroxypropyl acrylate, and DMA = *N,N*-dimethylacrylamide.

the LCST. These aggregates decrease in size at lower concentrations and become less dense and contain more water if more hydrophilic monomers are incorporated.[52,70,72] Possibly, the size of the aggregates formed by hydrophobic interchain interactions decreases with repeating heating cycles and becomes too small to be detected with turbidimetry. Alternatively, the ester bond of HPA can be subject to hydrolysis, causing increased hydrophilicity. As a test, aqueous copolymer solutions that were heated to 100 °C for 10 h and became transparent were freeze-dried and analyzed with ^{1}H NMR in DMSO-d_6. However, no acidic groups could be detected at ~12.4 ppm, indicating that no significant hydrolysis occurred. Further investigations on the specific hydrogen bonding interactions and aggregate size may help to identify the cause for this cycle effect.

Conclusions

The kinetics of the nitroxide-mediated homopolymerizations of 2-hydroxypropyl acrylate, *N,N*-dimethylacrylamide, and *N*-acryloylmorpholine were investigated with BlocBuilder alkoxyamine initiator and different percentages of SG-1 nitroxide. Best control over the polymerizations was observed for all three monomers at a reaction temperature of 110 °C in DMF using 20% additional SG-1. With these reaction conditions, two copolymer libraries were prepared on the basis of HPA and Amor or DMA with low polydispersity indices from 1.16 to 1.32. The copolymer compositions were analyzed by ^{1}H NMR spectroscopy and elemental analysis and were within 5% of the monomer feed. The glass transition temperatures and the LCST behavior of the copolymers were studied as a function of the monomer composition. Single glass transitions were observed for all polymers in both libraries, indicating good mixing of the monomers. Weak hydrogen-bonding interactions were detected for P(DMA-*stat*-HPA) as the T_g revealed a positive deviation from the Fox equation. The T_g of P(Amor-*stat*-HPA) could be related to the weight fraction via the Fox equation and did not show any specific interactions. The cloud points could be tuned in a range of 20−100 °C for both libraries. Increasing the hydrophilic monomer content increased the LCST, and the somewhat more hydrophilic DMA monomer caused a slightly sharper increase of the LCST. Copolymers with a high cloud point, due to a low concentration or a high hydrophilic content, showed an increased solubility with the number of heating cycles. The effect of the thermal history is still the subject of investigation but is most likely related to reduced hydrophobic interactions in the polymer aggregates and/or the formation of smaller aggregates.

In conclusion, we could systematically study the thermal transitions and LCST properties as a function of copolymer composition of two newly synthesized hydroxypropyl acrylate containing copolymer libraries. As such, HPA might be added to the rather limited number of monomers that can be used to prepare well-defined copolymers with a tunable LCST in aqueous solution.

Acknowledgment. The authors thank the Dutch Polymer Institute for financial support and Chemspeed Technologies A.G. for the collaboration. Arkema is thanked for providing BlocBuilder initiator and SG-1.

References and Notes

(1) Taylor, L. D.; Cerankowski, L. D. *J. Polym. Sci.* **1975**, *13*, 2551–2570.
(2) Gil, E. S.; Hudson, S. M. *Prog. Polym. Sci.* **2004**, *29*, 1173–1222.
(3) De las Heras Alarcón, C.; Pennadam, S.; Alexander, C. *Chem. Soc. Rev.* **2004**, *34*, 276–285.
(4) Kondo, A.; Ohnishi, N.; Furukawa, H. *Pharm. Tech. Jpn.* **2003**, *19*, 1753–1762.
(5) Lynch, I.; Blute, I. A.; Zhmud, B.; Macartain, P.; Tosetto, M.; Allen, L. T.; Byrne, H. J.; Farrell, G. F.; Keenan, A. K.; Gallagher, W. M.; Dawson, K. A. *Chem. Mater.* **2005**, *17*, 3889–3898.
(6) Costioli, M. D.; Fisch, I.; Garret-Flaudy, F.; Hilbrig, F.; Freitag, R. *Biotechnol. Bioeng.* **2003**, *81*, 535–545.
(7) Kikuchi, A.; Okano, T. *Prog. Polym. Sci.* **2002**, *27*, 1165–1193.
(8) Schmaljohann, D. *Adv. Drug Delivery Rev.* **2006**, *58*, 1655–1670.
(9) Bergbreiter, D. E.; Case, B. L.; Liu, Y.-S.; Caraway, J. W. *Macromolecules* **1998**, *31*, 6053–6062.
(10) Okhapkin, I. M.; Makhaeva, E. E.; Khokhlov, A. R. *Adv. Polym. Sci.* **2006**, *195*, 177–210.
(11) Lokuge, I.; Wang, X.; Bohn, P. *Langmuir* **2007**, *23*, 305–311.
(12) Wu, G.; Li, Y.; Han, M.; Liu, X. *J. Membr. Sci.* **2006**, *283*, 13–20.
(13) Fournier, D.; Hoogenboom, R.; Thijs, H. M. L.; Paulus, R. M.; Schubert, U. S. *Macromolecules* **2007**, *40*, 915–920.

(14) Jana, S.; Rannard, S. P.; Cooper, A. I. *Chem. Commun.* **2007**, 2962–2964.
(15) Meredith, J. C.; Amis, E. J. *Macromol. Chem. Phys.* **2000**, *201*, 733–739.
(16) Schild, H. G. *Prog. Polym. Sci.* **1992**, *17*, 163–249.
(17) Aoshima, S.; Kanaoka, S. *Adv. Polym. Sci.* **2008**, *210*, 169–208.
(18) Christova, D.; Velichkova, R.; Loos, W.; Goethals, E. J.; Du Prez, F. *Polymer* **2003**, *44*, 2255–2261.
(19) Perera, D. I.; Shanks, R. A. *Polym. Int.* **1995**, *37*, 133–139.
(20) Mori, H.; Iwaya, H.; Nagai, A.; Endo, T. *Chem. Commun.* **2005**, 4872–4874.
(21) Wang, J. S.; Matyjaszewski, K. *Macromolecules* **1995**, *28*, 7901–7910.
(22) Kamigaito, M.; Ando, T.; Sawamoto, M. *Chem. Rev.* **2001**, *101*, 3689–3746.
(23) Chiefari, J.; Chong, Y. K.; Ercole, F.; Krstina, J.; Jeffery, J.; Le, T. P. T.; Mayadunne, R. T. A.; Meijs, G. F.; Moad, C. L.; Moad, G.; Rizzardo, E.; Thang, S. H. *Macromolecules* **1998**, *31*, 5559–5562.
(24) Barner-Kowollik, C.; Davis, T. P.; Heuts, J. P. A.; Stenzel, M. H.; Vana, P.; Whittaker, M. *J. Polym. Sci., Part A: Polym. Chem.* **2003**, *41*, 365–375.
(25) Veregin, R. P. N.; Georges, M. K.; Hamer, G. K.; Kazmaier, P. M. *Macromolecules* **1995**, *28*, 4391–4398.
(26) Fukuda, T.; Terauchi, T.; Goto, A.; Ohno, K.; Tsujii, Y.; Miyamoto, T.; Kobatake, S.; Yamada, B. *Macromolecules* **1996**, *29*, 6393–6398.
(27) Braunecker, W. A.; Matyjaszewski, K. *Prog. Polym. Sci.* **2007**, *32*, 93–146.
(28) Matyjaszewski, K.; Gnanou, Y.; Leibler, L. *Macromolecular Engineering*; Wiley-VCH: Weinheim, Germany, 2007.
(29) Grimaldi, S.; Le Moigne, F.; Finet, J.-P.; Tordo, P.; Nicol, P.; Plechot, M. PCT WO 96/24620, Aug 15, 1996.
(30) Grimaldi, S.; Finet, J.-P.; Le Moigne, F.; Zeghdaoui, A.; Tordo, P.; Benoit, D.; Fontanille, M.; Gnanou, Y. *Macromolecules* **2000**, *33*, 1141–1147.
(31) Gigmes, D.; Bertin, D.; Guerret, O.; Marque, S. R. A.; Tordo, P.; Chauvin, F.; Couturier, J.-L.; Dufils, P.-E. PCT WO 2004/014926, Feb 13, **2004**.
(32) Hawker, C. J.; Bosman, A. W.; Harth, E. *Chem. Rev.* **2001**, *101*, 3661–3688.
(33) Le Mercier, C.; Acerbis, S.; Bertin, D.; Chauvin, F.; Gigmes, D.; Guerret, O.; Lansalot, M.; Marque, S.; Le Moigne, F.; Fischer, H.; Tordo, P. *Macromol. Symp.* **2002**, *182*, 225–247.
(34) Chauvin, F.; Dufils, P.-E.; Gigmes, D.; Guilaneuf, Y.; Marque, S. R. A.; Tordo, P.; Bertin, D. *Macromolecules* **2006**, *39*, 5238–5250.
(35) Nicolas, J.; Charleux, B.; Guerret, O.; Magnet, S. *Macromolecules* **2004**, *37*, 4453–4463.
(36) Nicolas, J.; Dire, C.; Mueller, L.; Belleney, J.; Charleux, B.; Marque, S. R. A.; Bertin, D.; Magnet, S.; Couvreur, L. *Macromolecules* **2006**, *39*, 8274–8282.
(37) Dire, C.; Charleux, B.; Magnet, S.; Couvreur, L. *Macromolecules* **2007**, *40*, 1897–1903.
(38) Nicolas, J.; Charleux, B.; Guerret, O.; Magnet, S. *Angew. Chem., Int. Ed.* **2004**, *43*, 6186–6189.
(39) Lacroix-Desmazes, P.; Lutz, J.-F.; Chauvin, F.; Severac, R.; Boutevin, B. *Macromolecules* **2001**, *34*, 8866–8871.
(40) Vo, C.-D.; Rosselgong, J.; Armes, S. P. *Macromolecules* **2007**, *40*, 7119–7125.
(41) Lizotte, J. R.; Long, T. E. *Macromol. Chem. Phys.* **2004**, *205*, 692–698.
(42) Bian, K.; Cunningham, M. F. *Macromolecules* **2005**, *38*, 695–701.
(43) Eeckman, F.; Moës, A. J.; Amighi, K. *Eur. Polym. J.* **2004**, *40*, 873–881.
(44) Favier, A.; Charreyre, M.-T.; Chaumont, P.; Pichot, C. *Macromolecules* **2002**, *35*, 8271–8280.
(45) Favier, A.; Charreyre, M.-T.; Pichot, C. *Polymer* **2004**, *45*, 8661–8672.
(46) De Lambert, B.; Charreyre, M.-T.; Chaix, C.; Pichot, C. *Polymer* **2007**, *48*, 437–447.
(47) Appelt, M.; Schmidt-Naake, G. *Macromol. Chem. Phys.* **2004**, *205*, 637–644.
(48) Mueller, K. F. *Polymer* **1992**, *33*, 3470–3476.
(49) Karaky, K.; Billon, L.; Pouchan, C.; Desbrières, J. *Macromolecules* **2007**, *40*, 458–464.
(50) Nichifor, M.; Zhu, X. X. *Polymer* **2003**, *44*, 3053–3060.
(51) Liu, H. Y.; Zhu, X. X. *Polymer* **1999**, *40*, 6985–6990.
(52) Barker, I. C.; Cowie, J. M. G.; Huckerby, T. N.; Shaw, D. A.; Soutar, I.; Swanson, L. *Macromolecules* **2003**, *36*, 7765–7770.
(53) Cao, Y.; Zhu, X. X.; Luo, J.; Liu, H. *Macromolecules* **2007**, *40*, 6418–6488.
(54) Bosman, A. W.; Vestberg, R.; Heumann, A.; Fréchet, J. M. J.; Hawker, C. J. *J. Am. Chem. Soc.* **2003**, *125*, 715–728.
(55) Diaz, T.; Fischer, A.; Jonquières, A.; Brembilla, A.; Lochon, P. *Macromolecules* **2003**, *36*, 2235–2241.
(56) Schierholz, K.; Givenchi, M.; Fabre, P.; Nallet, F.; Papon, E.; Guerret, O.; Gnanou, Y. *Macromolecules* **2003**, *35*, 5995–5999.
(57) Phan, T. N. T.; Maiez-Tribut, S.; Pascault, J.-P.; Bonnet, A.; Gerard, P.; Guerret, O.; Bertion, D. *Macromolecules* **2007**, *40*, 4516–4523.
(58) Fijten, M. W. M.; Kranenburg, J. M.; Thijs, H. M. L.; Paulus, R. M.; van Lankvelkt, B. M.; de Hullu, J.; Springintveld, M.; Thielen, D. J. G.; Tweedie, C. A.; Hoogenboom, R.; Schubert, U. S. *Macromolecules* **2007**, *40*, 5879–5886.
(59) Hoogenboom, R.; Schubert, U. S. *J. Polym. Sci., Part A: Polym. Chem.* **2003**, *41*, 2425–2434.
(60) Becer, C. R.; Paulus, R. M.; Hoogenboom, R.; Schubert, U. S. *J. Polym. Sci., Part A: Polym. Chem.* **2006**, *44*, 6202–6213.
(61) Bian, K.; Cunningham, M. F. *J. Polym. Sci., Part A: Polym. Chem.* **2006**, *44*, 414–426.
(62) Harth, E.; Van Horn, B.; Hawker, C. J. *Chem. Commun.* **2001**, 823–824.
(63) Acerbis, S.; Bertin, D.; Boutevin, B.; Gigmes, D.; Lacroix-Desmazes, P.; Le Mercier, C.; Lutz, J.-F.; Marque, S. R. A.; Siri, D.; Tordo, P. *Helv. Chim. Acta* **2006**, *89*, 2119–2132.
(64) Fox, T. G. *Bull. Am. Phys. Soc.* **1956**, *1*, 123–124.
(65) Young, R. J.; Lovell, P. A. *Introduction to Polymers*, 2nd ed.; Chapman & Hall: London, 1991; p 298.
(66) Kyeremateng, S. O.; Amado, E.; Kressler, J. *Eur. Polym. J.* **2007**, *43*, 3380–3391.
(67) Kuo, S.-W.; Liu, W.-P.; Chang, F.-C. *Macromolecules* **2003**, *36*, 5165–5173.
(68) Idziak, I.; Avoce, D.; Lessard, D.; Gravel, D.; Zhu, X. X. *Macromolecules* **1999**, *32*, 1260–1263.
(69) Tong, Z.; Zeng, F.; Zheng, X. *Macromolecules* **1999**, *32*, 4488–4490.
(70) Aseyev, V.; Hietala, S.; Laukkanen, A.; Nuopponen, M.; Confortini, O.; Du Prez, F.; Tehnu, H. *Polymer* **2005**, *46*, 7118–7131.
(71) Wang, X.; Qiu, X.; Wu, C. *Macromolecules* **1998**, *31*, 2972–2976.
(72) Maeda, T.; Yamamoto, K.; Aoyagi, T. *J. Colloid Interface Sci.* **2006**, *302*, 467–474.
(73) Hoogenboom, R.; Thijs, H. M. L.; Wouters, D.; Hoeppener, S.; Schubert, U. S. *Soft Matter* **2008**, *4*, 103–107.

MA800469P